Egypt. J. Chem. **Vol. 63,** No. 5, pp. 1619 - 1638 (2020)

Egyptian Journal of Chemistry
http://ejchem.journals.ekb.eg/

Synthesis of High Efficient CS/PVDC/TiO_2-Au Nanocomposites for Photocatalytic Degradation of Carcinogenic Ethidium Bromide in Sunlight

Amr A. El-Ella[1], Ahmed M. Youssef[2]*, Hala E. Ghannam[3], Abdallah F. Zedan[1], Wael M. Aboulthana[4] and Al-Sayed A. Al-Sherbini[1]

[1]Department of Measurements, Photochemistry and Agriculture Applications, National Institute of Laser Enhanced Science (NILES), Cairo University, Giza, Egypt.
[2]Packaging Materials Department, National Research Centre, 33 El-Bohouth St. (former El-Tahrirst.), Dokki, Giza, P.O 12622, Egypt.
[3]Pollution Laboratory, National Institute of Oceanography and Fisheries, Egypt.
[4]Biochemistry Department, Genetic Engineering and Biotechnology Division, National Research Centre, 33 El-Bohouth St.(former El-Tahrirst.), Dokki, Giza, P.O 12622, Egypt.

ETHIDIUM bromide (EtBr) is one of the most broadly used dyes in molecular biology laboratories. It was considered a strong mutagenic, carcinogenic and possesses a major safety problem for the researchers and environmental hazards during the disposal process. In the current study chitosan (CS) and polyvinylidene chloride (PVDC) based on different morphologies of TiO_2-Au nanocomposites were prepared, namely as CS/PVDC/TiO_2-Au nanocomposites. Firstly, titanium dioxide nanowires (TiO_2-NWs) and gold nanoparticles (Au-NPs) as well as TiO_2-NWs modified by Au-NPs (Au/TiO_2) nanocomposites were successfully prepared. Au/TiO_2 nanocomposite was fabricated and evaluated using X-ray diffractometer (XRD) and transmission electron microscope (TEM). Furthermore, chitosan was prepared from crabs shell wastes and blended with PVDC. The different loading of Au/TiO_2 nanocomposites were incorporated onto the nanocomposites thin films. The prepared CS/PVDC/TiO_2-Au nanocomposites films were characterized using UV-Visible spectra, Fourier transforms infrared (FT-IR), XRD and TEM. Moreover, the CS/PVDC/TiO_2-Au nanocomposites were used for photodecomposition of EtBr under sunlight irradiation from~ 400-600 W/m^2 with and without aeration as well as assaying integrity of the EtBr after decomposition by horizontal gel electrophoresis. The results established that the CS/PVDC/TiO_2-Au nanocomposites were sufficient to remove ~70-90 % of the EtBr through the irradiated time course and ~ 60 % of the dye was degraded in the first one hour.

Keywords: Chitosan; TiO_2 NWs; Au NPs; Thin-film; Ethidium Bromide; Nanocomposites; Gel Electrophoresis.

Introduction

Photocatalytic degradation is a process that occurs as a result of the interaction of the photocatalyst and irradiated light that yields a highly reactive radical like, O^-_2, H_2O_2, OH, OH^-, O_2, HO_2, and HO^-_2. All of these radicals having high levels of reactivity and became the main species responsible for the advanced oxidation and reduction processes of the pollutants. It is well known that the pollution of water and soil with pollutant materials can lead to serious diseases such as cancer and have

*Corresponding author e-mail: amyoussef27@yahoo.com
Tel/ Fax, (202) 33322418 (202) 33370931, P.C. 12622
Received 5/1/2020; Accepted 29/1/2020
DOI: 10.21608/ejchem.2020.21987.2313

gained worldwide attention due to the serious effects on living organisms. Amongst these serious pollutants, ethidium bromide (EtBr) has been considered a strong mutagenic, carcinogenic and possesses a major safety problem when it is released to the environment [1].

Ethidium bromide (EtBr) is a dark-red cationic dye, nonvolatile and moderately soluble in water. The dye consists of four aromatic rings and three of these aromatic rings can provide strong and specific interaction with double-stranded DNA and RNA via intercalation between base pairs [2, 3]. Therefore, Ethidium bromide dye is widely utilized as a fluorescent label in biological and medical laboratories in the visualization of nucleic acid bands based on the gel-electrophoresis technique and other life science applications [4]. Being a causing carcinogenic agent, EtBr contaminated wastes are recommended to be decontaminated or treated before its disposal. The removal of ethidium bromide from the surroundings was carried out by many methods. Conventional methods rely on the treatment of polluted water with low concentrations of ~ 10-200 ppm with sodium hypochlorite (bleach) prior to its disposal to drainage [5]. However, such conventional methods may result in free radical formation and production of chloro-organic byproducts which may not be safe. Other methods for the removal of EtBr like activated charcoal, ion-exchange-resin, incineration and bioremediation which depends on the bacterial strains are applied. Heterogeneous photocatalytic approaches such as the advanced oxidation processes have received great attention as an active and efficient performance for the removal of organic pollutants from water under solar light illumination with minimal formation of hazard by-products [6].

Titanium dioxide (TiO_2) is one of the most studied photocatalyst materials for various photocatalytic applications such as the photocatalytic degradation of different toxic compounds including organic and inorganic water pollutants [7,8]. Furthermore, TiO_2 possesses redox properties favorable for both oxidations of organic pollutants and the reduction of several metal ions [9,10]. However, the properties of TiO_2 must be modified to enhance energy conversion efficiency. However, the large band gap of TiO_2 (3.2 eV) limits it light absorption to only 5% of the solar spectrum. Thus, exploration of how can TiO_2 be modified to achieve sensitization to visible light of the solar spectrum energy is a significant requisite. In addition, aqueous powder dispersions of TiO_2 suffer from several drawbacks associated with the cost of separating TiO_2 from the water after treatment either by sedimentation or ultrafiltration.

To overcome these obstacles recent work on TiO_2 photocatalysis has been directed towards the immobilization of TiO_2 as thin films [11]. The immobilization and stabilization method eliminates most of the problems associated with slurries such as particle aggregation and enables the development of self-cleaning and self-sterilizing surfaces [12]. Moreover, numerous attempts to improve the catalytic performance of TiO_2 have included, among other methods, modification with noble metals. Most such efforts have been centered on Pt/TiO_2 systems [13], although a limited number of studies on the Au/TiO_2 and Ag/TiO_2 systems have also been reported [14].

Correspondingly, to reduce the limitations of TiO_2 comprising the wide optical bandgap (3.21 eV for anatase) and charge carrier recombination, the heterojunction with noble metals such as gold (Au) has been shown as a promising strategy to improve the light-harvesting and catalytic properties of TiO_2. The noble metals such as gold (Au) nanoparticles can act as electron trapping centers in addition to the plasmon coupling provided by the strong absorption band of Au nanoparticles in the visible region of the electromagnetic field at around 520 nm. This plasmon absorption results from the collective oscillation of free electrons at the metal surface, which is called the surface plasmon resonance (SPR) [15].

In the present work, we have been designed and fabricated thin-films of chitosan/polyvinylidene chloride supported with TiO_2 nanoparticles and, TiO_2 nanowires or TiO_2-Au nanocomposites via TiO_2-NPs and, TiO_2-NWs. The photocatalytic activity of the prepared thin films for photocatalytic decomposition of ethidium bromide (EtBr) under solar energy has been investigated.

Materials and Methods

Materials

Polyvinylidene chloride (PVDC) (Biopolymer, USA), Titanium dioxide, TiO_2 (deggusa P25), Hydrochloric Acid (HCl), Sodium hydroxide (NaOH), Trisodium citrate, ($C_6H_5O_7Na_3$), Hydrogen Tetrachloroaurate trihydrate ($HAuCl_4$),

Ethidium bromide (EtBr), Acetonitrile, Acetic acid (CH_3COOH), were obtained from, Aldrich, (Puriss). Agarose gel electrophoresis was obtained from Sigma Aldrich, (USA), Distilled water (Nanopure) produced by millipore instrument.

Methods

Extraction of chitosan from crabs shell wastes

Extraction of chitosan from the crab's shells wastes was obtained from the local markets and suspended in 4 % HCl at 25^{0}C in the ratio of 1:14 (w/v) up to 36 h and the residual was washed with water to remove acid and calcium chloride. The deproteinization of shells was done by treating the residual with 5 % NaOH at 90°C for 24 h with a solvent to solid ratio of 12:1 (v/w). After the incubation time the shells were washed with running tap water and sun dried, the product obtained was chitin. Chitosan produced by deacetlyation of obtained chitin [16]. By employing 70 % NaOH solution with a solid to liquid ratio of 1:14 (w/v) and incubated at 25 ^{o}C for 72 h. The residue obtained after 72 h washed with running tap water and rinsed with deionized water. The product was sun dried and finely grinded to the powder chitosan.

Preparation of TiO_2 nanowires

TiO_2 nanowires (TiO_2-NWs) were prepared by the hydrothermal treatment of anatase TiO_2 powder with concentrated KOH solution followed by acid treatment in HCl solution. Classically, 2 g of anatase TiO_2 particles was added to 40 mL of 10 M KOH aqueous solution in a 100 ml Teflon vessel. The mixture was stirred for 30 min and then the Teflon-lined stainless steel autoclave was transferred to an electric oven and kept at 140°C for 48 h. After the hydrothermal treatment, the precipitate was separated by filtration and washed three times with deionized water. Then, the precipitate was soaked in an aqueous solution for 2 h at room temperature after adjusting the pH to 6 with 0.1 M HCl. Finally, the precipitate was separated by filtration and dried in an oven at 80°C overnight. Dried samples were calcined for 2 h at 450°C with a heating ramp rate of 5° C min^{-1}.

Preparation of gold nanoparticles (Au-NPs)

Gold nanoparticles were fabricated using sodium citrate as reducing agent according to the following procedure: 1 ml of $5x10^{-3}$ mol dm^{-3} $HAuCl_4$ was added to 90 ml double distilled water. The solution was heated until boiling, and then 5 ml of 0.5 % sodium citrate solution dropwise was added. As soon as boiling commences. The heating of the solution was kept until to the color changes from yellow to pale purple color due to formation of Au-NPs. Finally the heating was stopped and the mixture was continued stirring until cooled at room temperature 25^{o}C and then the mixture was completed to 100 ml by the distilled water.

Preparation of Au/TiO_2 nanocomposites

1 gm of TiO_2 nanoparticles (P25, Degussa), with about 30 nm cross-sectional dimension, was suspended in 90 ml of double distilled water in 250 ml conical flask. Then 5 ml of 0.5 % sodium citrate solution was added. As soon as boiling of the mixture started, 1 ml of $5x10^{-3}$ mol dm^{-3} $HAuCl_4$ was added drop wisely with continues stirring. The heating was continued until the color changed from colorless to pink color due to the formation of Au-NPs deposited on the surface of TiO_2. The surface modification and stabilization by Au-NPs described as Au/TiO_2-(nanoparticles and nanowire) nanocomposites association with increase the property of surface to size ratios of TiO_2 photocatalyst. The heating was turning off with continuous stirring to more 15 min. then, the prepared nanocomposites were separated by filtration and drying at 60^{o}C.

Preparation of CS/PVDC based on TiO_2-(nanoparticles or nanowires) thin films

20 mg of TiO_2-(nanoparticles powder and prepared nanowires) was added to 80 ml of stocked solution of 0.64 % chitosan (CS) and 20 ml of biopolymer polyvinylidene chloride (PVDC) was mixed then, sonication the mixture for 10 min, and suspended into plastic plates with dimensions of 15x20 cm to obtain the desired concentrations of CS/PVDC/TiO_2-(nanoparticles powder and prepared nanowires) nanocomposites thin films. The plates were dried at room temperature 25^{o}C 24 h to get the thin films with thickness were measured by digital micrometer gauge about 0.1 mm.

Preparation of CS/PVDC based on TiO_2-Au nanocomposites thin films

80 ml of stocked solution of 0.64 % CS was added to 20 ml of PVDC and the mixture were mixed with 20 mg of TiO_2/Au nanocomposites and by sonication the mixture for 10 min, and poured the composites into vessels or plates with dimensions of 15x20 cm to obtain the desired concentrations of CS/PVDC/TiO_2-Au nanocomposites thin films. The plates were dried to get the thin films with thickness about 0.1 mm.

Characterizations

Measurement of electronic absorption spectra

UV-visible absorption spectra were measured using *Perkin Elmer Lambda 40* double beam spectrophotometer, using matched quartz cells with 1 cm path length and the absorption was recorded within the appropriate scan range.

Transmission electron microscopy (TEM)

Transmission electron microscopy of the samples was formed by drying a drop of the solution on a carbon-coated copper grid. Particle sizes were determined from the micrographs of the Joel-100S transmission electron microscope, of resolution of 0.3 nm.

X-ray diffraction analysis (XRD)

A crystallographic study was performed on the samples powder by Rotating Anode X-ray Diffractometer (Rigaku, Japan) using Cu Ka radiation. The distances between peaks, D; were calculated according to Scherrer's equation and were compared to the JCPDS file 2.532X-ray diffraction (XRD) data to deduce the crystal structure.

Fourier-transform infrared measurements (FT-IR)

Fourier-transform infrared (FT-IR) measurements were obtained using Perkin Elmer-2000. Before measurement, 1 mg of the sample was mixed with 200 mg KBr to make a disc for FT-IR absorption measurement. The spectra were collected in the scanning range of 450 to 4000 cm^{-1} with a resolution of 1 cm^{-1}.

Assaying integrity of ethidium bromide (EtBr)

Integrity of EtBr was examined using genomic DNA extracted from liver tissue of rats according protocol suggested by *Barker et al*. [17]. The DNA purity and concentration were determined by NanoDrop Spectrophotometer (Thermo Scientific NanoDrop Products) which is designed for measuring nucleic acid concentrations in sample volumes of one microliter. Absorbance was measured at wavelengths of 260 and 280 (A_{260} and A_{280}, respectively) nm. An absorbance quotient value of 1.8 < ratio (R) < 2.0 was considered to be good and accepted, purified DNA. A ratio of < 1.8 is indicative of protein contamination; where as a ratio of > 2.0 indicates RNA contamination.

Equal concentrations of the genomic DNA mixed with equal volume of EtBr (whether standard and hydrolysate solution). Integrity of the EtBr was assayed using gel electrophoresis (Bio-Rad, USA) by resolving DNA extracts on a 1.5 % agarose without EtBr. The DNA bands that were visualized on a UV transilluminator indicated to integrity of EtBr that still able to interact with DNA molecule. The gel was photographed by Gel Documentation System then analyzed in comparison to DNA molecular weight marker (HyperLadder II) with regularly spaced bands ranging from 50 bp to 2000 bp. The DNA bands in agarose gel were analyzed using Quantity One software (Version 4.6.2). The relative mobility (Rf), band intensity (Int.) and quantity (Quant.) in addition to the molecular weights of the electrophoretically detected DNA bands were determined.

Results and Discussion

Morphological investigation of the prepared nanomaterials as well as the prepared CS/PVDC/TiO_2-Au nanocomposites using TEM.

Figure 1 illustrates photograph of TiO_2-NPs, TiO_2-NWs, Au/TiO_2NPs, Au/TiO_2-NWs and the CS/PVDC/TiO_2-Au nanocomposites thin films. Fig.1 (a) displayed that the homogenous spherical shape of TiO_2 nanoparticles with average size ~ 10±2 nm. While Figurer 1b revealed that the TEM micrographs of TiO_2 nanowires, the image suggests that (i) the bundled TiO_2 nanowires mostly stay in a stacked (i.e. one sitting on the other) and warped form due to an interfacial bonding that holds all the nanowires together in a bundle, and (ii) the recognizable space in between the nanowires in the bundles is due to the interfacial bonding as weak as, likely a H-bonding. Furthermore, the fabricated gold nanoparticles deposited onto the surfaces of TiO_2 displayed as Au/TiO_2NPs, as well as Au/TiO_2-NWs were demonstrated in Fig.1(c and d) as highly dispersed black dots with average size ~ 18.38±2 nm, onto the surfaces of TiO_2-(nanoparticles and nanowires). As observed in (Fig.1 e), the prepared CS/PVDC/TiO_2-Au nanocomposites thin film was bound on or embedded by the fabricated Au/TiO_2 nanocomposites in the thin film.

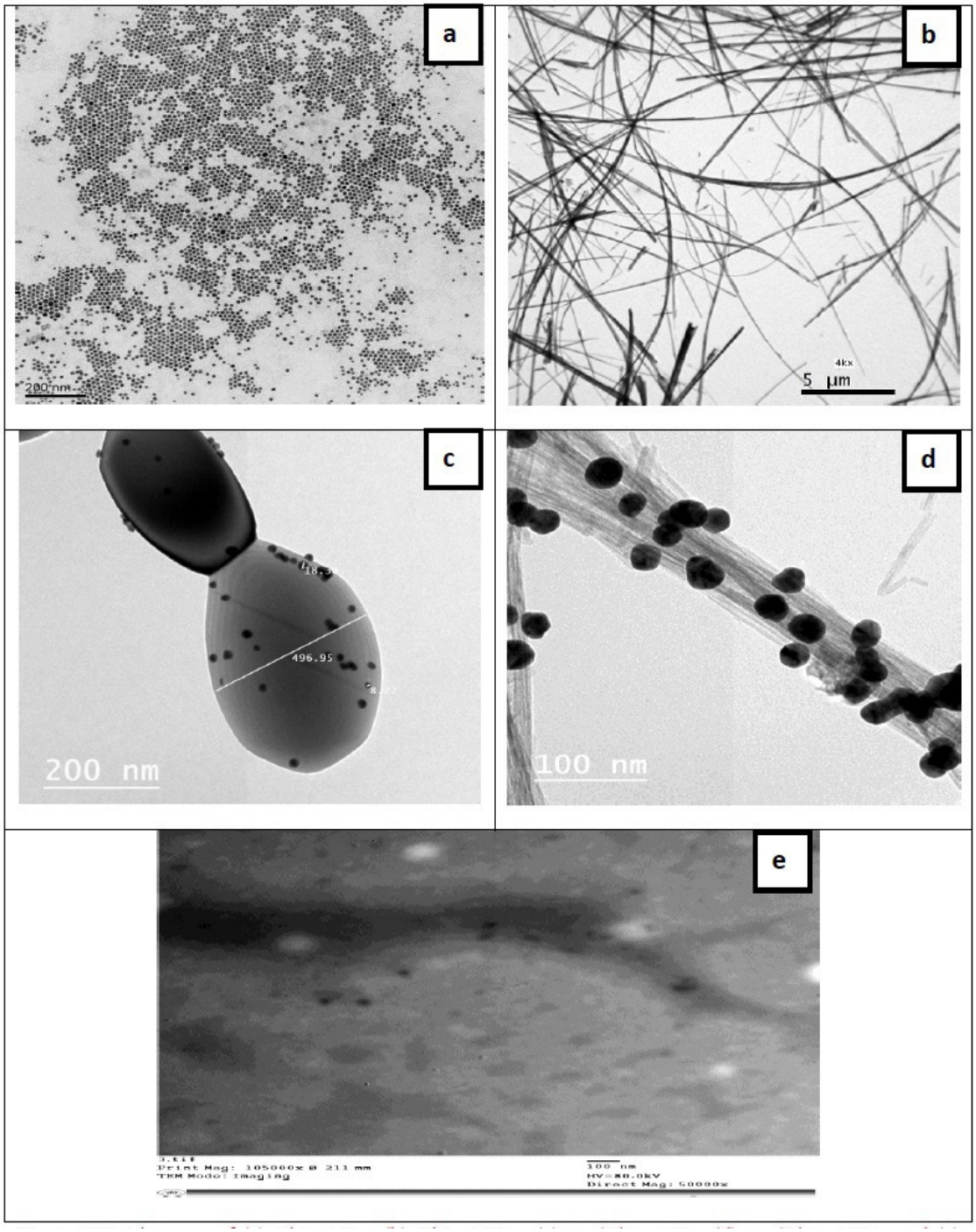

Fig.1. TEM images of (a) TiO_2-NPs, (b) TiO_2-NWs, (c) Au/TiO_2-NPs, (d) Au/TiO_2-NWs and (e) CS/PVDC/TiO_2-Au nanocomposites.

UV–Visible absorption spectra of the prepared nanomaterials

UV–Visible absorption spectra of gold, titanium dioxide nanoparticles, TiO_2/Au nanocomposites are shown in **Fig.** 2. The Figure displays the optical absorption spectra of 18.38 ± 2 nm gold nanoparticles with an intense band at $\lambda_{max.}$ = 528 nm and assignable to the surface plasmon resonance (SPR) band. On the other hand TiO_2-NPs show maximum absorption spectra at $\lambda_{max.}$ = 298 nm. In addition the spectral measurements are carried out to establish the presence of Au-NPs on TiO_2 nanoparticles which allocated the maximum absorption spectra at λ_{max}= 316 nm in case of core TiO_2-NPs and 526 nm for TiO_2/Au-NPs, respectively. This leads to the higher photocatalytic activity under UV-Visible light.

X-Ray Diffraction Analysis (XRD)

TiO_2 nanoparticles and nanowires

The X-ray diffraction pattern of the synthesized titanium dioxide nanoparticles is shown in **Fig. 3** (a and b) and the peak of the (101), (116), (103), (200), (213), (105) and (107) crystal planes of anatase were selected to determine the lattice parameters. This corresponds to 2θ at 25.80°, 38.4°, 48.01°, 54.7°, 63.0°, 69.3° and 75.8°, respectively as demonstrated in (Fig. 3a) details are in the experimental XRD pattern agrees with the JCPDS card no. 21-1272 (anatase TiO_2) and the XRD pattern of TiO_2 nanoparticles other literature. The 2θ at peak 25.8°and 48.01° confirms the TiO_2 anatase structure. The diffraction peaks at 2Θ of 25.80° and 48.01° are ascribed to the crystallographic structure anatase phase indicating TiO_2 in the anatase phase [18]. There is no any spurious diffraction peak found in the sample. The 2θ peaks at 25.8° and 48.01° confirm its anatase structure.

The intensity of XRD peaks of the sample reflects that the formed nanoparticles are crystalline and broad diffraction peaks indicate very small size crystallite. In case of TiO_2 nanowires (Fig.3b), the characteristic diffraction peaks at 2θ= 25.3°, 37.8°, 48°, 53.5°, 55.6°, 62.7° and 75° correspond well to the (101), (004), (200), (105), (211), (204) and (215) planes, respectively. The sharp diffraction peaks of four XRD patterns demonstrate the good crystalline of synthesized TiO_2 nanowire structure. The highly crystallized nanostructure can reduce the opportunity of charge recombination, which improves the photocatalytic performance [19].

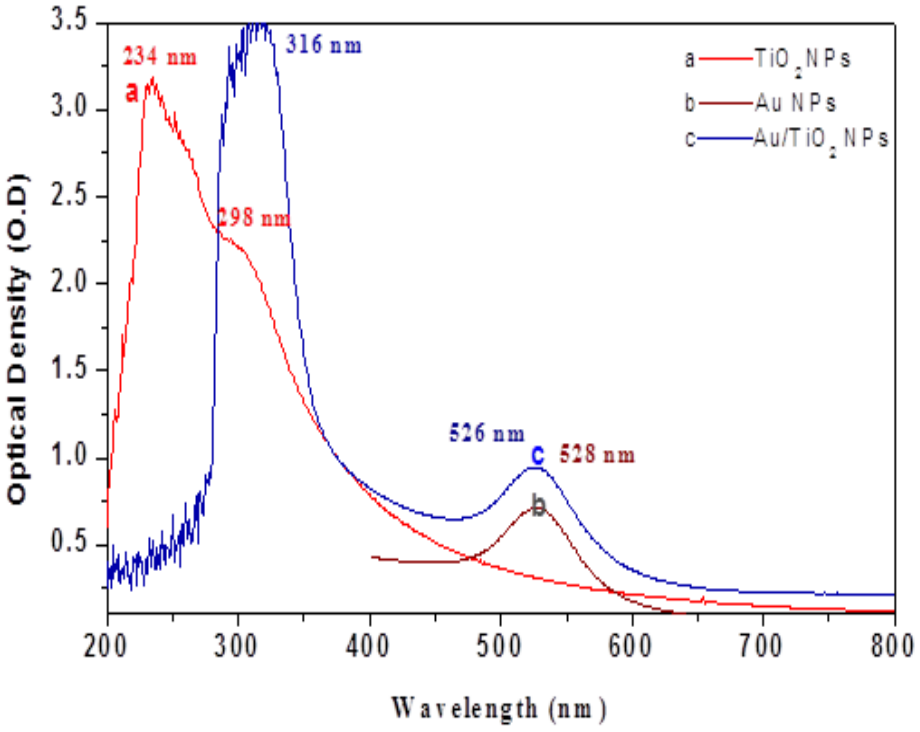

Fig. 2. Optical absorption spectra of Au-NPs, TiO_2-NPs and Au/TiO_2 nanocomposites.

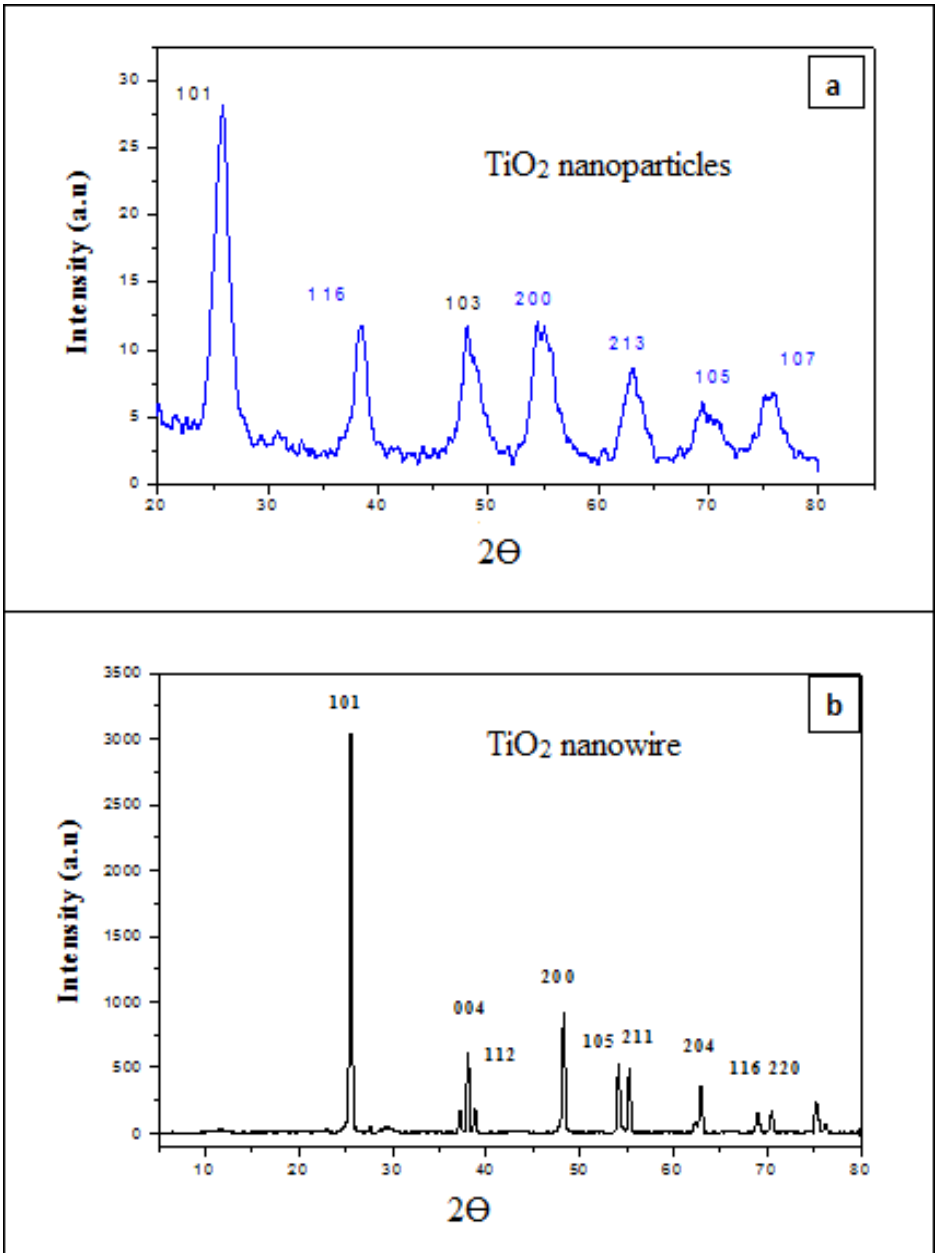

Fig. 3. XRD pattern of a) TiO_2 nanoparticles, b) TiO_2 nanowires.

Fourier-transform infrared measurements (FT-IR)

FT-IR Spectra of TiO_2 nanoparticles, Au/TiO_2-NPs nanocomposite, TiO_2 nanowires and Au/TiO_2-NWs nanocomposite are shown in **Fig.** 4 (a-d). In case of Fig.4a, TiO_2 nanoparticles it clearly shows three bands. The first band is broadest and observed at 3500 cm^{-1} corresponding to the stretching vibration of the hydroxyl group OH. The second band is observed around 1615 cm^{-1}, corresponding to bending modes of water Ti-OH, the last is a prominent peak at 1451 cm^{-1} related to Ti-O modes [20] in the case of TiO_2 nanowires.

It was observed from Fig.4b that the nanowires were having characteristic peaks in the range of 500–700 cm^{-1} and 995 cm^{-1} which are assigned to the Ti–O–Ti and Ti-O stretching vibrations. The bond Ti–OH observed below 3400 cm^{-1} indicates the existence of hydrogen bonding and attributed to the OH spectral region. To study the influence of noble metal capping to TiO_2 nanowires, Fig.4 c showed that two characteristic bands at 3793 and 3685 cm^{-1} were detected in the OH spectral region between 3400–4000 cm^{-1}.

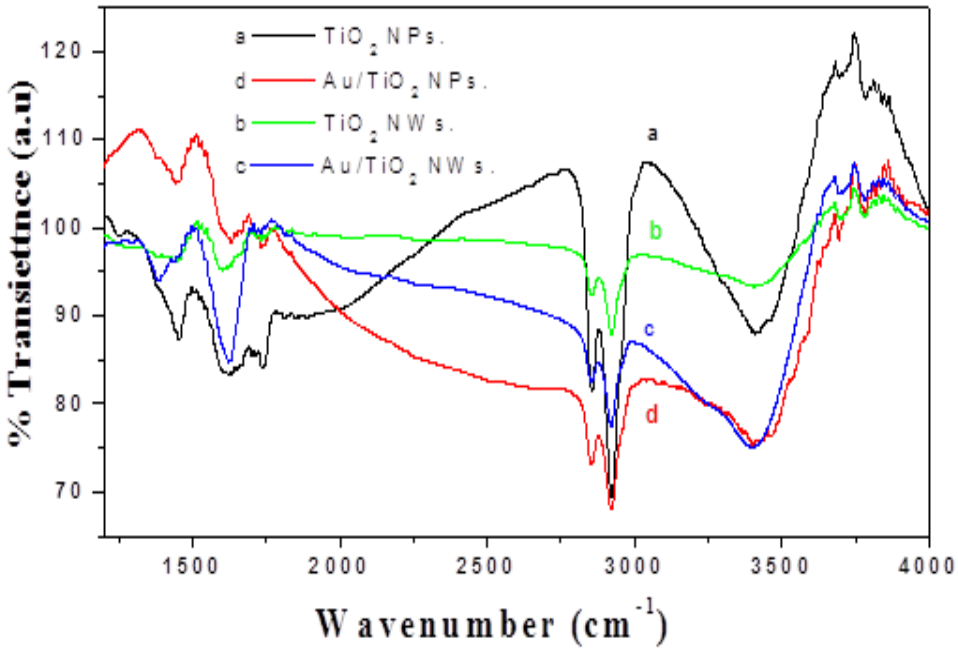

Fig. 4. FT-IR spectra of a) TiO_2-NPs b) TiO_2-NWs c) TiO_2-NWs-Au-NPs and d) TiO_2-NPs-Au-NPs.

The shift was observed in the Figure due to the presence of Au loaded TiO_2 nanowires, also the absorbance bands of 1625 cm^{-1}, 1390 cm^{-1} and 750 cm^{-1} indicated the presence of molecular functional groups that are responsible for the reduction of gold ions. In the case of TiO_2-Au nanocomposites two characteristic bands at 3693 and 3632 cm^{-1} were detected in the OH spectral region between 3400–4000 cm^{-1}, in (Fig.4d) the higher frequency band is ascribed to terminal hydroxyl groups coordinated to Ti^{+4} sites, which enhance the photocatalytic activity of Au/TiO_2 nanocomposites [21].

Photocatalytic Experiments

Photocatalysis was carried out in sunlight or solar energy between 10 AM and 2 PM during the summer days and the average sunlight intensity was 400-600 W/m^2 measured by Eldonet instruments. The photocatalysis experiment was carried out by illuminating 250 ml of aqueous sample of ethidium bromide in the basic form at ~ pH = 12 and operational temperature was at 25°C. Control experiments were carried out without light in the presence of TiO_2-(nanoparticles or nanowires) thin films and into Au/TiO_2-(nanoparticles or nanowires) thin films. The experiment was carried out in the presence of sunlight without using the nanocomposites thin films.

The experiment was carried in the presence and absence of oxygen for all the photocatalysis experiments. Samples (3 ml) were taken out at regular time (~30 min) intervals, to monitoring the degradation activity by using a UV-visible double beam spectrophotometer. **Fig. 5** demonstrated that the electronic absorption spectra of 3x 10^{-5} mole dm^{-3} of ethidium bromide dye. Figure (5-1) displayed that the basic form of ethidium bromide assigned $\lambda_{max.}$ = 479±2 nm, Fig. (5-2) indicated that in a dark experiment about (15 %) of ethidium bromide adsorbed on the TiO_2 surface of thin films after 2 h. This attributed to adhesion of dye and leads to the higher photocatalytic activity under UV-Visible sunlight.

Furthermore, slightly degradation of the ethidium bromide in the control sample after 2 h irradiation in the sunlight about (20 %) of the dye was degraded without thin film (Fig. (5-3), in addition, the presence of surface plasmon resonance band of gold nanoparticles at 528 nm, gold NPs, at $\lambda_{max.}$= 526 nm, and the maximum absorption band of the basic form at 479±2 nm might enhance the photocatalytic activity. The thin films have a thickness ~ 0.1 mm which exhibit interesting optical properties due to the interference of sunlight as it reflects through the materials [22].

Photodegradation of CS/PVDC nanocomposites based on TiO_2-NPs (with and without) aeration.

In the current study used UV-Visible sunlight or solar energy for photocatalytic degradation of the aqueous solution of ethidium bromide, Fig. 6 revealed that the absorption spectra of ethidium bromide solution at different time intervals over 20 mg of TiO_2-NPs thin films without aeration. The figure illustrated that, the optical density at $\lambda_{max.}$ = 479±2 nm gradually decreases with increasing the time courses up to 240 min. The basic medium, pH = 12 enhanced formation of OH, because at high pH about 12 more hydroxide groups available on TiO_2 anatase (P25) surface can be easily oxidized to radical form OH^-, more OH which consequently increases the radical efficiency of degradation. It is shown that, during irradiation time, the characteristic absorption band of the dye at $\lambda_{max.}$= 479 ±2 nm decreased without new absorption bands appeared, this might be due to that the ethidium bromide dye had photodegradation activity without the formation of intermediate molecules.

It was observed from the result that ~ 72 ± 2 % of ethidium bromide dye without aeration, was degraded in 4 h. In the presence of aeration it was observed that increasing the photocatalytic efficiency of the TiO_2 nanoparticles owing to increasing the oxygen content in the medium associated with increasing the photocatalytic degradation rate of ethidium bromide dye. **Fig. 7** demonstrated the absorption spectra at different degradation time courses with aeration. In this study, the air was introduced in the system by the use of the peristaltic pump and this tends that, the oxygen content in the aquatic system increases and accompanying with increasing of OH radicals which are responsible for the photodegradation of ethedium bromide. The figure displays that, after irradiation time to 240 min, about 75 % of the dye was degraded over TiO_2 nanoparticles polymer thin film.

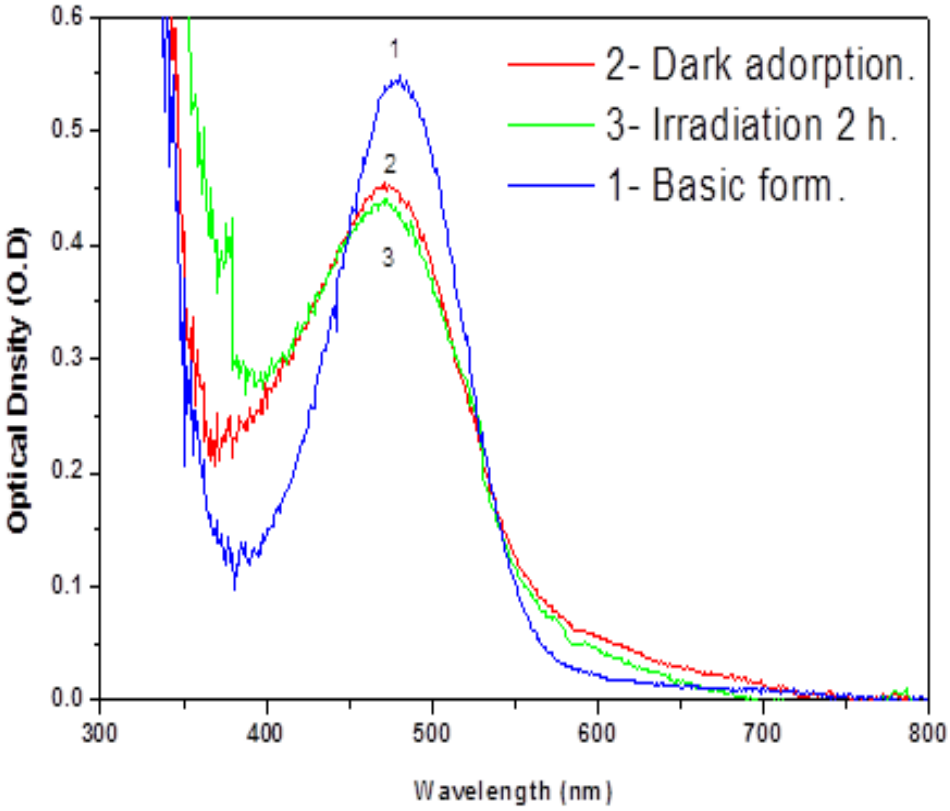

Fig. 5. The electronic absorption spectra changes of, 1) Basic form, 2) Dark adsorption, 3) Irradiation 2 h of solution ethidium bromide 3x 10^{-5} mole dm^{-3}

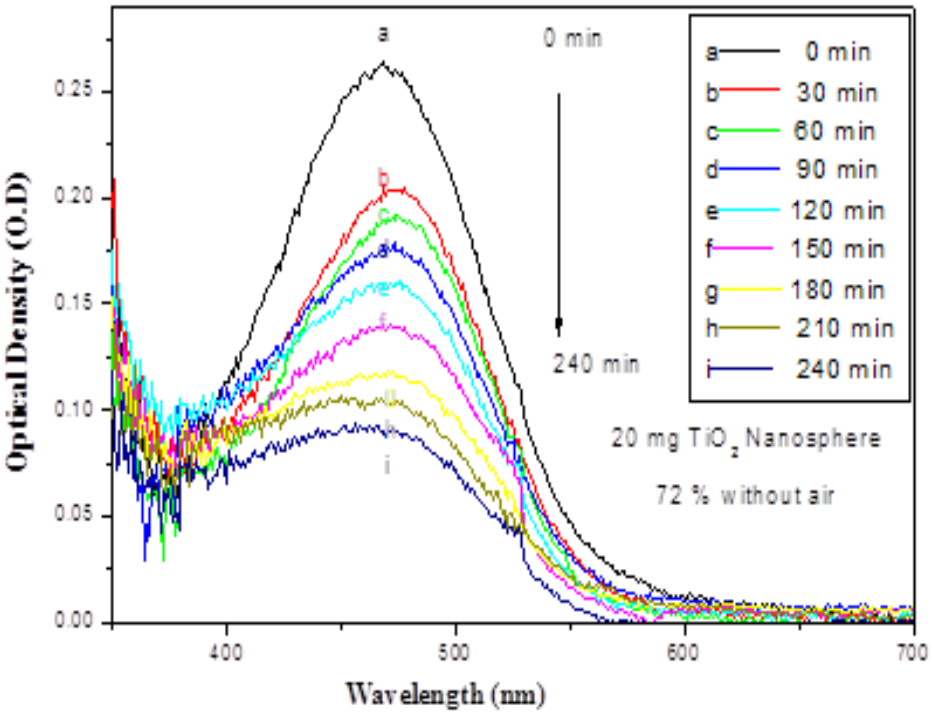

Fig. 6. UV-visible Absorption spectra of $3x10^{-5}$ mole dm^{-3} of ethidium bromide irradiated at different time intervals with sunlight irradiation on CS/PVDC nanocomposites thin films based on TiO_2-NPs without aeration.

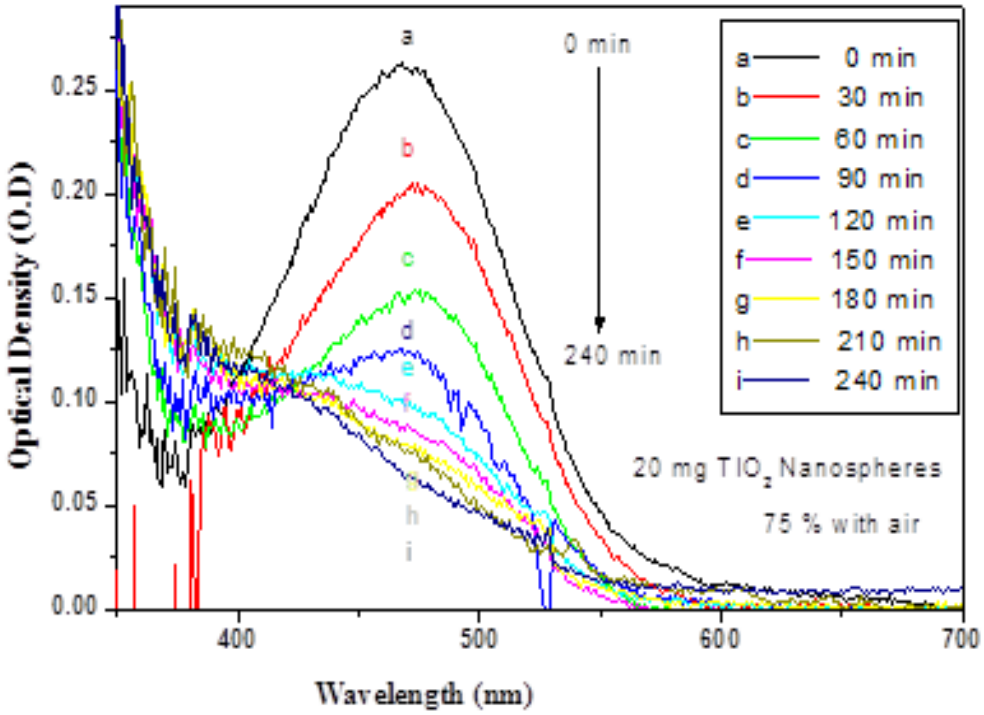

Fig. 7. UV-visible Absorption spectra of $3x10^{-5}$ mole dm^{-3} of ethidium bromide irradiated at different time intervals with sunlight irradiation on CS/PVDC nanocomposites thin films based on TiO_2-NPs thin films with aeration.

Photodegradation of CS/PVDC nanocomposites thin films based on TiO_2-NPs/Au (with and without) aeration

For improving the photocatalytic performance of TiO_2 nanoparticles via modification with the noble metals such as Au nanoparticles to form TiO_2-Au nanocomposites system, the presence of the plasmon band of gold nanoparticles at wavelength λ_{max}= 528 nm with a maximum position of ethidium bromide at wavelength $\lambda_{max.}$= 479 ± 2 nm may enhances the photocatalytic activity of UV-Visible sunlight. Au nanoparticles can be considered as an electron sink, preventing the recombination electron-hole pairs of TiO_2 and by the way, it enhance the production of OH radicals in the surrounded environment.

Additionally under visible-sunlight irradiation, Au nanoparticles are photoexcited through the surface plasmon resonance (SPR) of Au absorption and the excited electrons are injected into the surrounding and in this case, the production of all radicals are accelerated, which eventually accelerates the photodegradation rate of ethidium bromide dye. It was observed from **Fig. 8** that the disappearance rate decreases gradually with irradiation time and the photodegradation rate of ethidium bromide dye after irradiation to 240 min, in the absence of oxygen was about 77% on the thin film.

In the presence of air flow and under irradiation of UV-Visible sunlight, the aquatic solution of ethidium bromide over TiO_2-Au nanocomposites thin film, shows increasing in the photocatalytic degradation as shown in **Fig. 9**. The increasing in the degradation rate might be owing to the driving of more oxygen content in the system. As illustrated in the **Figure** after irradiation to 240 min, about 88 % of the dye was degraded over CS/PVDC thin film based on TiO_2-Au nanocomposites.

Photodegradation of CS/PVDC nanocomposites thin film based on TiO_2-NWs (with and without) aeration

Generally, the specific surface area and light absorption ability are two essential factors, which can significantly influence the photocatalytic activity of the photocatalysts, TiO_2 nanowires having a high surface-to-size ratio, which contributes to the excellent adsorption capacity. The large surface area of the photocatalysts allows more surface to be reached by the incident light and provides more reactive sites during the photodegradation process in the UV region and has shown to reduce electron-hole pair recombination and increase photocatalytic efficiency [23]. In the existing experiment, the effect of 20 mg of TiO_2 nanowires embedded in polymer thin films without and with aeration for degradation the aqueous ethidium bromide was carried out. **Fig. 10** indicated that the photodegradation of ethidium bromide is about 77 % without aeration.

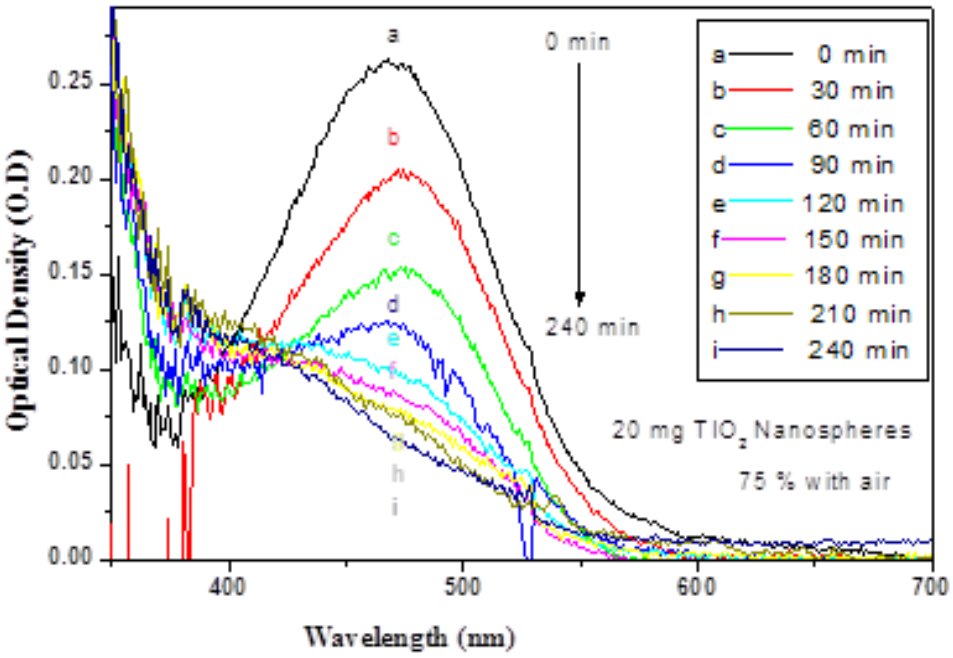

Fig. 8. UV-visible Absorption spectra of $3x10^{-5}$ mole dm^{-3} of ethidium bromide irradiated at different time intervals with sunlight irradiation on CS/PVDC nanocomposites thin films based on TiO_2-NPs/Au without aeration.

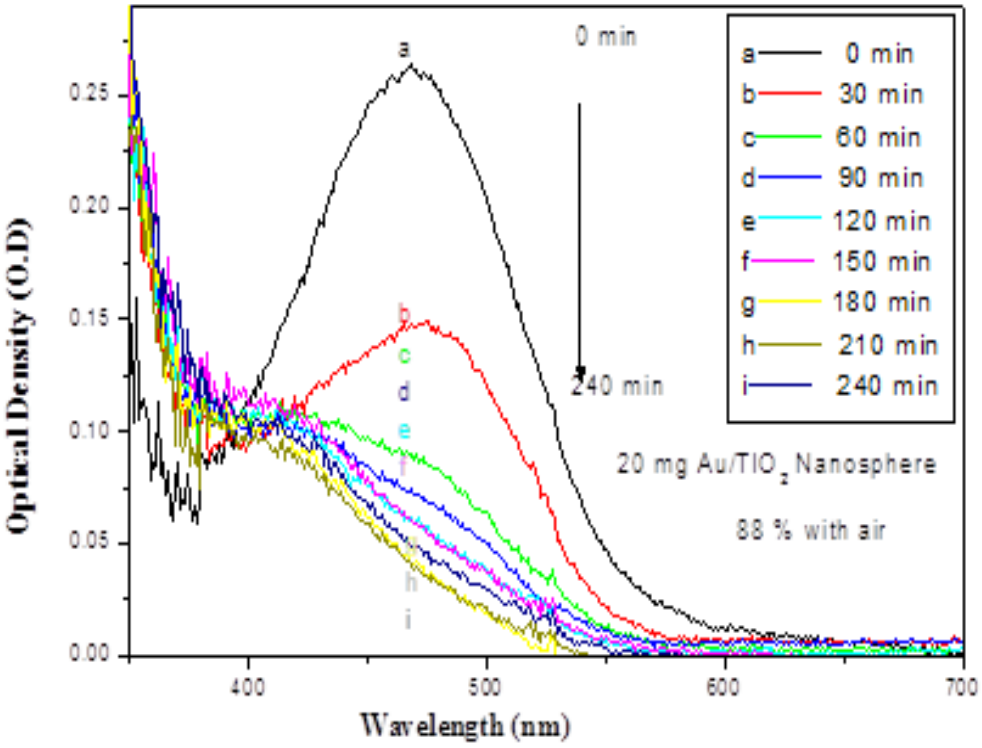

Fig. 9. UV-visible Absorption spectra of $3x10^{-5}$ mole dm^{-3} of ethiduim bromide irradiated at different time intervals with sunlight irradiation on CS/PVDC nanocomposites thin films based on 20 mg TiO_2-Au nanocomposites with aeration.

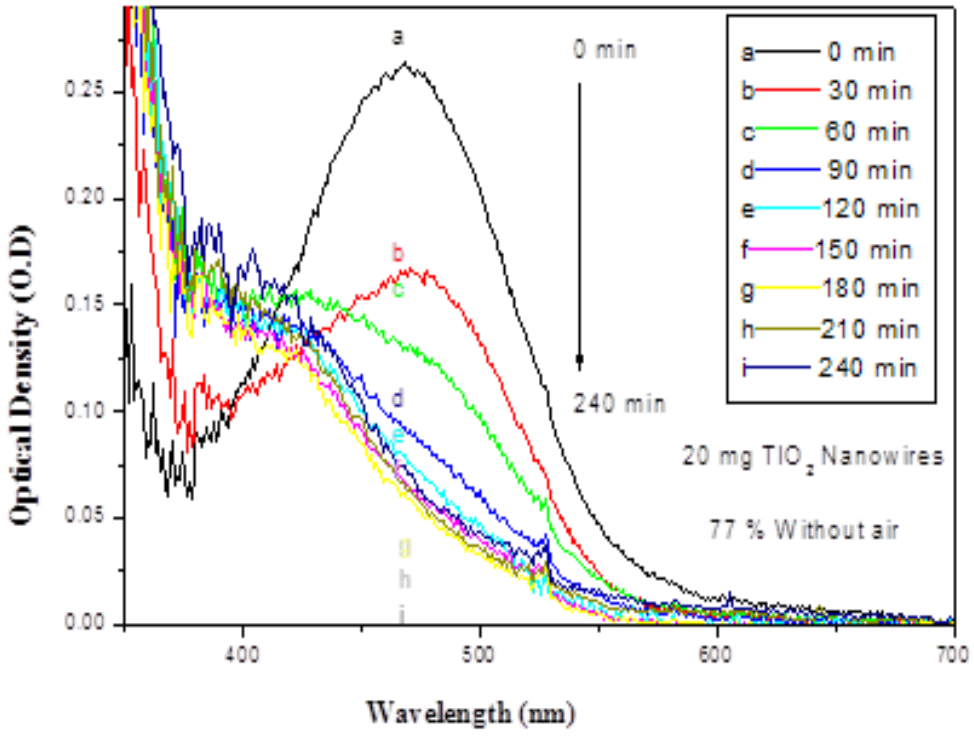

Fig. 10. UV-visible Absorption spectra of $3x10^{-5}$ mole dm^{-3} of ethidium bromide irradiated at different time intervals with sunlight irradiation on CS/PVDC nanocomposites thin film based on TiO_2-NWs without aeration.

As expected, the photodegradation rate of ethidium bromide increases in the case of TiO_2 nanowire more than the TiO_2 nanoparticles by ~ 5 %, with pumping of air flow in the presence of sunlight, **Fig. 11** displayed that the photodegradation percent of ethidium bromide was increased to about 85 % during the same time interval courses of 240 mines. As expected, the photodegradation rate of ethidium bromide increases in the presence of air flow by ~ 8 %, more than in the absence of air.

Photodegradation of CS/PVDC nanocomposites thin film based on TiO_2-NWs/Au (with and without) aeration

Several strategies aimed to extending the wavelength of photo-activation of TiO_2-(nanoparticles or nanowires), into the visible region of the electromagnetic spectrum to increase the utilization of sunlight preventing the electron-hole pairs recombination and thus allowing more charge carriers to successfully diffuse to the surface; increasing the adsorption affinity of TiO_2-(nanoparticles or nanowire) towards the pollutants. Noble metal nanoparticles such as Au have also been used to modify TiO_2 for photocatalysis and have been reported to efficiently hinder electron-hole pair's recombination due to the resulting schottky barrier at the metal-TiO_2 interface. In this state, noble metal nanoparticles act as a mediator in storing and transporting photogenerated electrons from the surface of TiO_2 to an acceptor. The photocatalytic activity increases as the charge carrier's recombination rate are decreased [24].

The present study was carried out in sunlight source without air flow on Au/TiO_2 nanowires composites polymer thin film illustrated in **Fig. (12)**, shows that after irradiation to 240 min about ~ 88 % of the dye was degraded over the thin films. As maintained up, the presence of plasmon band of gold nanoparticles λ_{max} = 528 nm and the absorption band of ethidium bromide in the visible region λ = 479±2 nm may enhance the photocatalytic activity of UV-Visible sunlight. When the oxygen introduced to the photoreactor nanosystem by using a peristaltic pump and irradiated to UV-Visible sunlight, **Fig. (13)**. The rate of photodegradation illustrated that after irradiation time course 240 min, about 90 % of the dye was degraded over the thin films. As expected, the photodegradation rate of ethidium bromide increases because of the presence of gold nanoparticles.

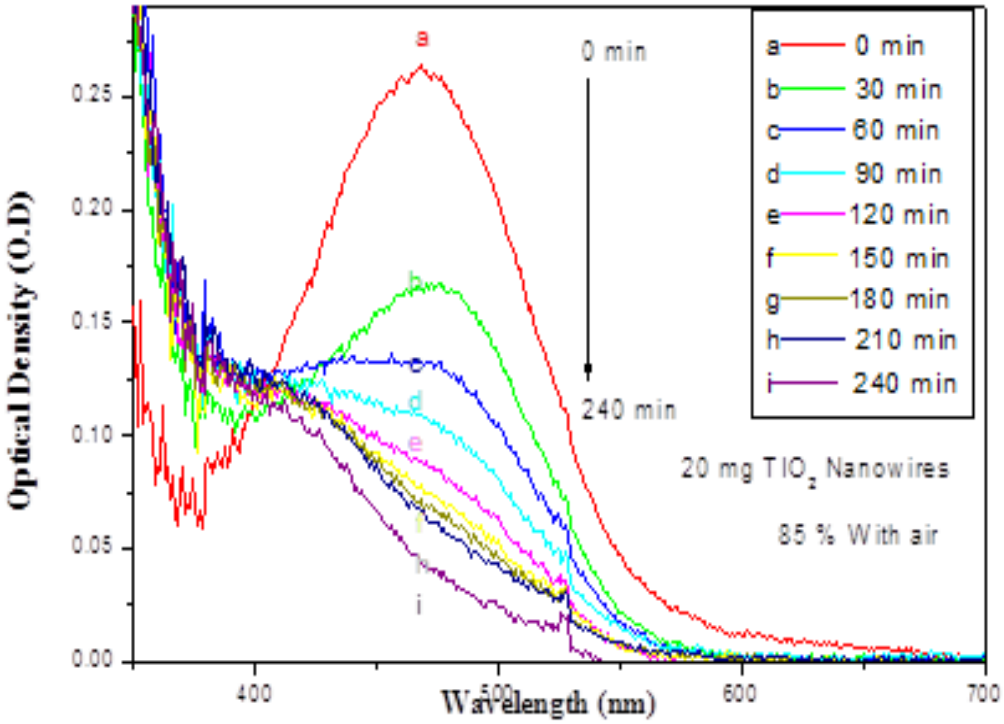

Fig. 11. UV-visible Absorption spectra of $3x10^{-5}$ mole dm^{-3} of ethidium bromide irradiated at different time intervals with sunlight irradiation on CS/PVDC nanocomposites thin films based on TiO_2-NWs with aeration.

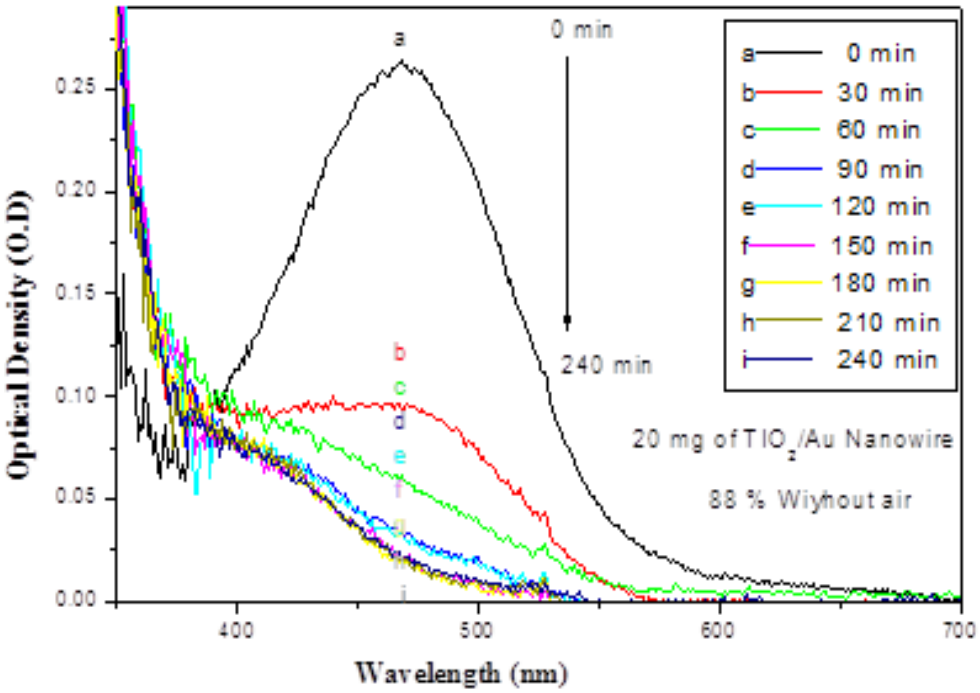

Fig. 12. UV-visible Absorption spectra of $3x10^{-5}$ mole dm^{-3} of ethidium bromide irradiated at different time intervals with sunlight irradiation on CS/PVDC nanocomposites thin films based on TiO_2-NWs/Au without aeration.

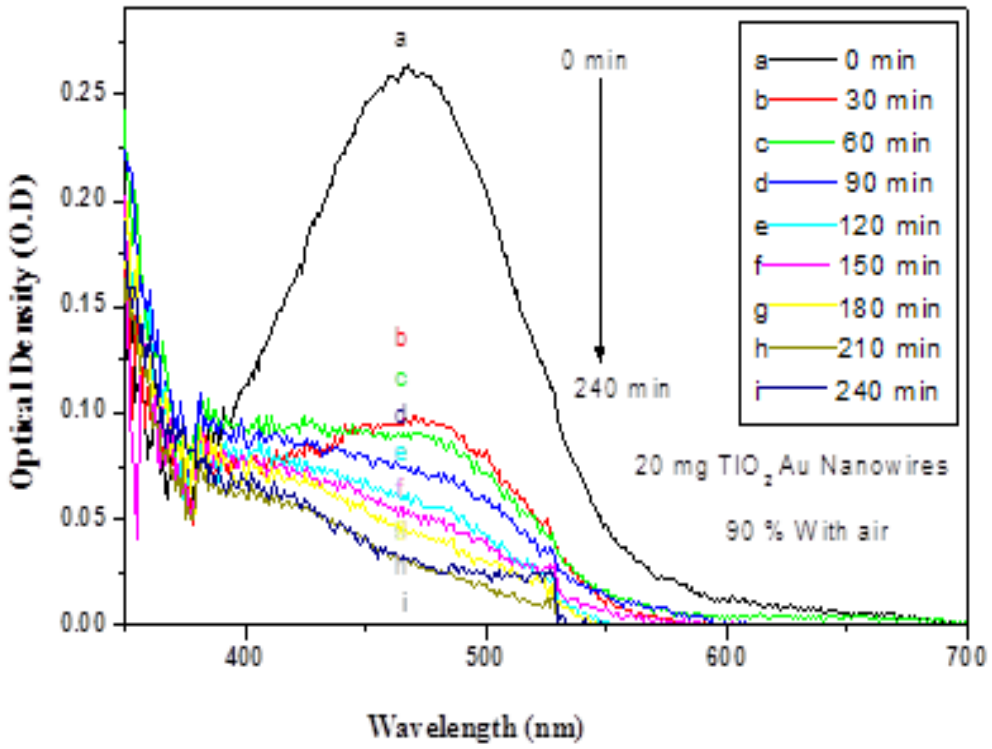

Fig. 13. UV-visible Absorption spectra of $3x10^{-5}$ mole dm^{-3} of ethidium bromide irradiated at different time intervals with sunlight irradiation on CS/PVDC nanocomposites thin films based on TiO_2-NWs/Au with aeration

Photodegradation rate of ethiduim bromide (with and without) aeration under irradiation of sunlight

Due to the higher photocatalytic activity under UV-Visible sunlight and accordingly the charge transfer between excited ethiduim bromide molecules and the system components to produce radicals were more efficient on the surface. The presence of the plasmon band of gold nanoparticles at wavelength λ_{max} = 528 nm and the absorption band of ethiduim bromide in the visible region at wavelength λ_{max} = 479±2 nm may enhances the photocatalytic activity of UV-Visible sunlight. In this study 20 mg of different morphologies of TiO_2 nanoparticles and nanowires), Au/TiO_2-(nanoparticles and nanowires) nanocomposites embedded in polymer thin films were used. The average rates of photodegradation were calculated according to the following equation:

$$\text{Rate} = (A_o - A/t) \quad (1)$$

Where; A_o is the concentration at zero time in mol dm^{-3}, A is the concentration at any time in mol dm^{-3}, t is the observed time in sec.

The normalized photodegradation of ethidium bromide on the irradiation time course is shown in Figure 14, Figure 15 and Scheme (1). The Figures shows that the photodegradation rates were in between (4-6) x 10^{-5} mol dm^{-3} sec^{-1} and the photodegradation % were from (72-88 %) without aerations. As observed in the Figures, the rates of decomposition assisted by TiO_2 sphere-gold nanocomposites, TiO_2 nanowire and Au/TiO_2 nanocomposites is much faster than the one catalyzed by CS/CDVC/TiO_2-Au nanocomposites thin film as shown in **(Figure 14).** while with aeration the rate of photodegradation via Au/TiO_2-NPs nanocomposites, TiO_2 nanowires and Au/TiO_2-NWs nanocomposites were in between (5-7) x10^{-5} mol dm^{-3} sec^{-1} and the photodegradation % were from (75-90 %), which is much faster than that catalyzed without aerations were displayed in **Fig. (15).**

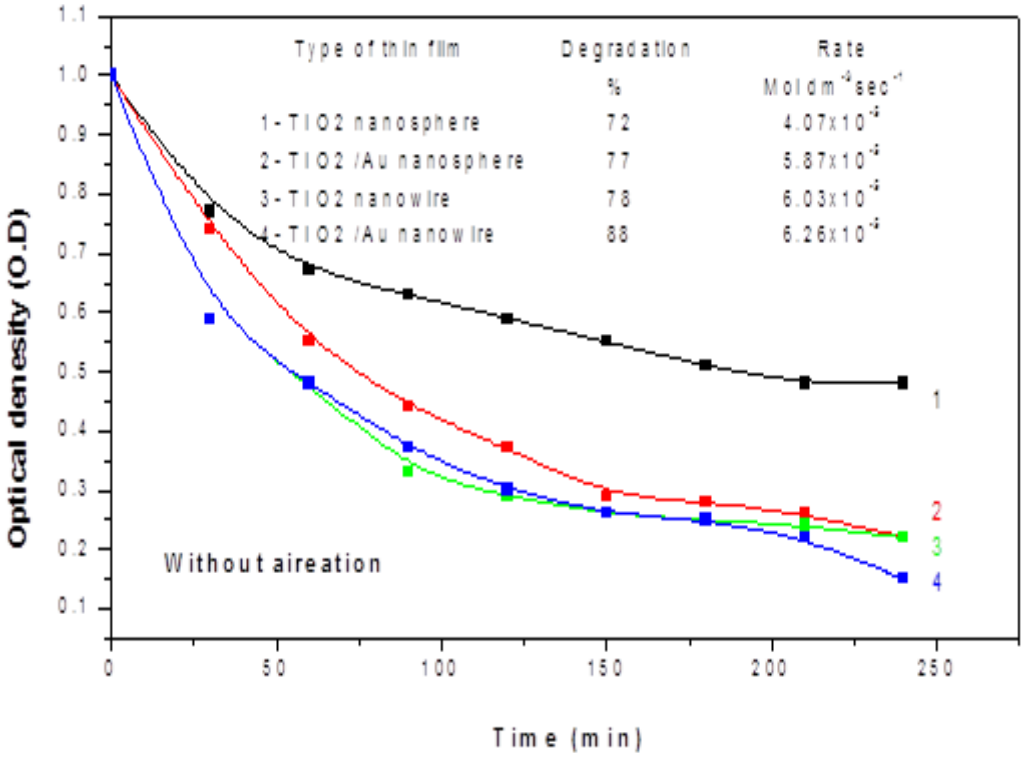

Fig. 14. Dependence of the normalized concentration of ethidium bromide as a function of irradiation time without aeration

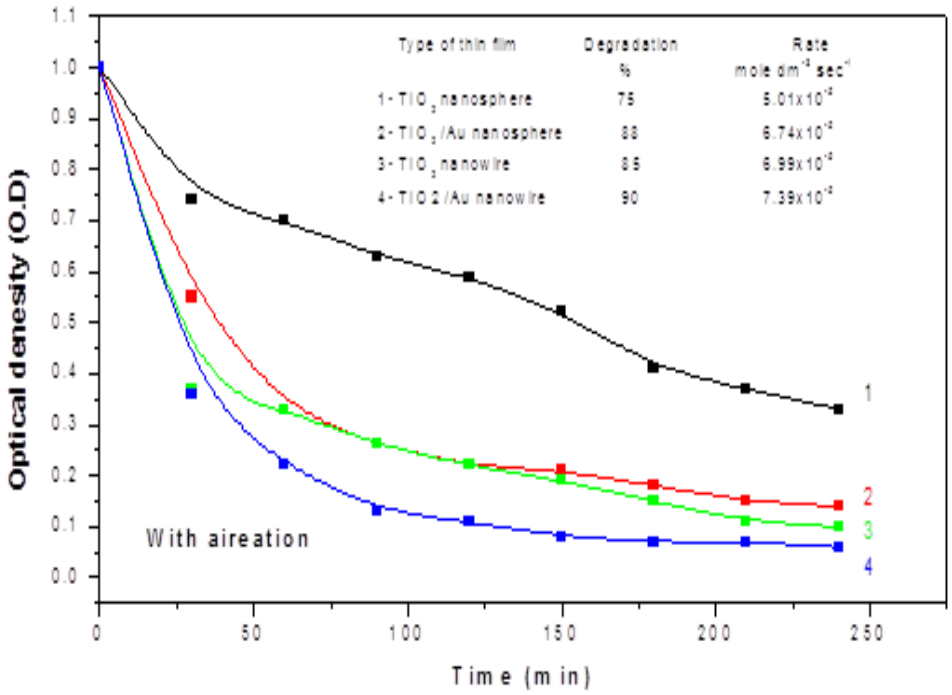

Fig. 15. Dependence of the normalized concentration of ethidium bromide as a function of irradiation time with aeration.

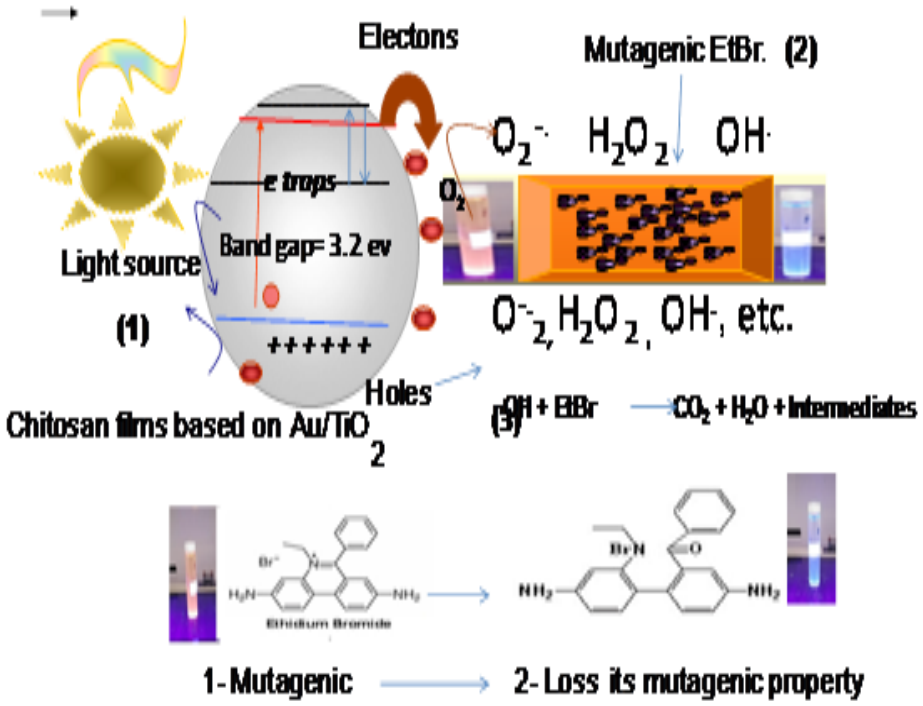

Scheme 1. Schematic changes in the electronic levels of Au/TiO_2 nanocomposites and the role of different radicals in photocatalytic decomposition of Ethidium Bromide.

Mechanism of ethidium bromide degradation

The possible mechanism of the photocatalytic decomposition of ethidium bromide in aqueous solution in the presence of TiO_2 or TiO_2-gold nanoparticles thin films by irradiation under sunlight is presented in Scheme (1). In photocatalytic decomposition, the catalyst absorbs photons and this leads to the excitation of electrons from the valence band to the conduction band, which generates electron-hole pairs. In this case all the system is under reduction oxidation processes. In the reduction process the electrons in the conduction band are captured by oxygen molecules that are dissolved in the medium to produces $\cdot O^-_2$, H_2O_2, $\cdot OH$, OH^-, O_2, HO_2 and, HO^-_2 radicals (2) according the following [25].

$$Ti\,O_2\,(e^-) + O_2 \longrightarrow TiO_2 + \cdot O^-_2$$

$$Ti\,O_2\,(e^-) + O_2 -. + 2H^+ \longrightarrow Ti\,O_2 + H_2O_2$$

$$Ti\,O_2\,(e^-) + H_2O_2 \longrightarrow Ti\,O_2 + OH^- + \cdot OH$$

$$\cdot O^-_2 + H2\,O_2 \longrightarrow OH^- + \cdot OH + O_2$$

$$\cdot O^-_2 + H^+ \longrightarrow H\,O_2$$

$$TIO2(e^-) + .HO_2 \longrightarrow TiO_2 + HO_2$$

$$\cdot HO_2 + .H^+ \longrightarrow H_2O_2$$

While in the oxidation process, the holes in the valence band can be captured by the H_2O or OH^- species that are adsorbed on the surface of the catalyst to produce $\cdot O^-_2$, H_2O_2, $\cdot OH$, OH^-, O_2, $\cdot HO_2$ and, HO^-_2 radicals(3) according the following.

$$Ti\,O_2\,(h^+) + H_2O \longrightarrow Ti\,O_2 + \cdot OH + H^+$$

$$Ti\,O_2\,(h^+) + 2H_2O_{Ads} \longrightarrow Ti\,O_2 + 2\,H^+ + H_2O_2$$

$$TiO_2\,(h^+) + OH\text{-}Ads \longrightarrow TiO_2 + \cdot OH$$

All of these radicals having high levels of reactivity and can readily initiate oxidation resulting in the degraded of ethidium bromide molecules. The addition of noble metals like Au on the TiO_2 nanoparticles increases the rate of formation of radicals and accordingly increasing the rate of photocatalytic decomposition. The presence of Au nanoparticles as a trap might be enhance the utilization of visible light by enhance the separation of photogenerated holes and electrons and decreases the electron hole recompilation. This leads to high photodegradation of ethidium bromide in visible light. In addition, in case of nanowire the surface area of the catalyst increases which increasing the radicals in the surrounding accompanying in increasing of the rate of the photodegradation by ~ 5 %.

Studying intercalating activity of ethidium bromide with genomic DNA after photodegradation process

The data revealed in Fig. (16 a) and illustrated graphically in Fig. (16 b) and compiled in Tables (1) showed that the standard EtBr reacted with the integrated genomic DNA that extracted from liver tissue of rats. In the presence of integrated EtBr, it was found that the genomic DNA expressed electrophoretically on agarose gel as one thick band identified at Rf. 0.200, Mwt 2353 BP, Int. 235.93 and Quant. 17.82%. This was in accordance with Tsuboi et al. (2007) [26], who reported that EtBr exhibited intercalating activity with genomic DNA. Moreover, they revealed the relative orientations of the phenanthridinium ring of EtBr and bases of DNA through studying the polarized spectra that showed the interaction between oriented specimens of EtBr (single crystal) and DNA (hydrated fiber) and it was found that the phenanthridinium ring and its immediate base neighbors have coplanarity ability at the intercalation site closer to A-DNA than B-DNA.

Furthermore, the EtBr hydrolyzed chemically and hence lost its ability to react with the genomic DNA. The genomic DNA expressed as one faint band identified at Rf. 0.197 and Mwt 2443 BP and hence the band Int. and Quant. % decreased to 36.50 and 1.19%, respectively. Therefore, the DNA could not be visualized completely after the electrophoretic separation and this was attributed to the loss of the fluorescence of EtBr after photodegradation process.

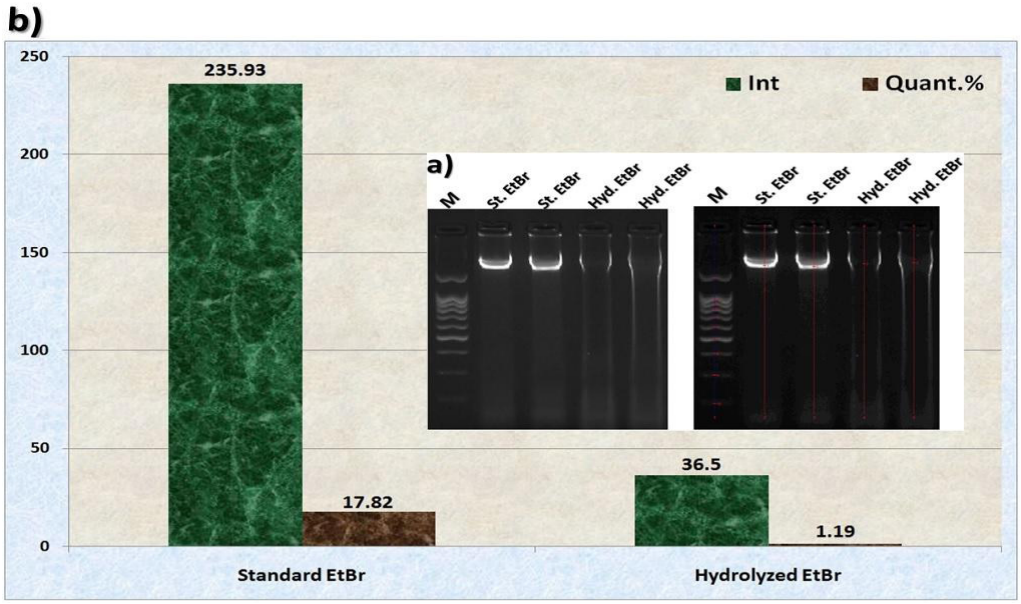

Fig. 16. Genomic DNA pattern showing effect of chemical hydrolysis on a) ability of Ethidium Bromide (EtBr) to react genomic DNA, b) intensity and quantity of the genomic DNA extracted from liver tissue of rats as compared to standard .

TABLE 1. showing the qualitative and quantitative data of the electrophoretically separated genomic DNA after its reaction with standard and hydrolyzed EtBr as compared to DNA marker.

Marker			
Rf.	Mwt. (BP)	Int.	Quant. %
0.266	2000	65	7.07
0.380	1500	98	10.01
0.409	1000	87.72	4.52
0.441	500	80.86	5.49
0.481	208	65	5.39
0.532	69	65	5.45
0.597	16	87.72	7.45
0.675	3	53.57	5.11
0.791	0.23	38.43	5.05
0.945	0.01	32	1.67

EtBr Standard				EtBr Standard				Mean Average			
Rf.	**Mwt. (BP)**	**Int.**	**Quant. %**	**Rf.**	**Mwt. (BP)**	**Int.**	**Quant. %**	**Rf.**	**Mwt. (BP)**	**Int.**	**Quant. %**
0.198	2372	253.72	18.21	0.201	2334	218.14	17.43	0.200	2353	235.93	17.82
EtBr hydrolyzed				**EtBr hydrolyzed**				**Mean Average**			
Rf.	**Mwt (BP)**	**Int.**	**Quant. %**	**Rf**	**Mwt. (BP)**	**Int.**	**Quant. %**	**Rf**	**Mwt. (BP)**	**Int.**	**Quant. %**
0.197	2423	32.00	1.07	0.197	2462	41.00	1.31	0.197	2443	36.50	1.19

Rf.: Relative Mobility, **Mwt. (BP)**: Molecular Wight by Base Pair, **Int.**: Band Intensity, **Quant. %**: Band Quantity %.

Conclusions

The surface modification and deposition of Au-NPs, on the surface lattice of TiO_2 (nanoparticles or nanowires) by thin-film method results in substitutional impurities with the retention of the nanocrystalline and anatase phases, which fine-tunes the electronic properties of TiO_2 resulting in the better utilization of a much broader spectrum of solar radiation. The studied composition shows that the creation of mid bands for effective charge separation together with the narrowing of the bandgap within the visible range facilitates an increase in catalytic activity of TiO_2 photocatalyst leading to the complete degradation of an ethidium bromide solution ($3x10^{-5}$ mole dm^{-3}) within 120 min of exposure to sunlight. The electrophoretic analysis confirmed the non-mutagenicity of the treated sample. Ethidium bromide, being a derivative of phenanthridium, easily succumbs to the sunlight-induced reactive oxygen species that are generated by the modified titania catalysts. We thus investigated a highly efficient procedure for the synthesis of gold-deposited on TiO_2 surface lattice and its application as a visible-light-induced photocatalyst for demutagenesis of mutagens. The novel and renewable thin film can be acquired for a longer time period.

References

1. Zhang, C., Liu, L., Wang, J., Rong, F., and Fu, D. Electrochemical degradation of ethidium bromide using boron-doped diamond electrode. Separation and Purification Technology, **107**, 91-101 (2013).
2. Machado, I.M. B. F. Study of the interactions between dna and ionic liquids (Doctoral dissertation, Universidad del País Vasco-Euskal Herriko Unibertsitatea) (2016).
3. Ge, Z., Sun, T., Xing, J., and Fan, X. Efficient removal of ethidium bromide from aqueous solution by using DNA-loaded Fe_3O_4 nanoparticles. Environmental Science and Pollution Research, **26**(3), 2387-2396 (2019).
4. Law, J. W. F., Ab Mutalib, N. S., Chan, K. G., and Lee, L. H. Rapid methods for the detection of foodborne bacterial pathogens: principles, applications, advantages and limitations. Frontiers in microbiology, **5,** 770 (2015).
5. Youssef, A. M., Malhat, F. M., Abdel Hakim, A. Dekany, I. Synthesis and utilization of poly (methylmethacrylate) nanocomposites based on modified montmorillonite. Arabian Journal of Chemistry 10, 631–642 (2017).
6. Rahimi, M. R., and Mosleh, S. Intensification of Textile Wastewater Treatment Processes. Advanced Textile Engineering Materials, 329-387 (2018).
7. Youssef, M.A., and Malhat, M. F. Selective Removal of Heavy Metals from Drinking Water Using Titanium Dioxide Nanowire, Macromol. Symp. 337, 96–101 (2014).
8. Lavand, A. B., and Malghe, Y. S. Visible-light photocatalytic degradation of ethidium bromide using carbon-and iron-modified TiO_2 photocatalyst. Journal of Thermal Analysis and Calorimetry, 123(2), 1163-1172 (2016).
9. Rufus, A., Sreeju, N., and Philip, D. Size tunable biosynthesis and luminescence quenching of nanostructured hematite (α-Fe_2O_3) for catalytic degradation of organic pollutants. Journal of Physics and Chemistry of Solids, 124, 221-234 (2019).
10. Youssef, M. A., Malhat, M. F., Abdelhakim, A. A. Preparation and Utilization of Polystyrene Nanocomposites based on TiO_2 nanowires, Polymer-Plastics Technology and Engineering, 52: 228–235 (2013).
11. Wang, Z., Wang, Y., Zhang, W., Wang, Z., Ma, Y., and Zhou, X. Fabrication of TiO_2 (B)/Anatase Heterophase Junctions at High Temperature via Stabilizing the Surface of TiO_2 (B) for Enhanced Photocatalytic Activity. The Journal of Physical Chemistry C, 123(3), 1779-1789 (2019).
12. Hebeish, A. A., Abdelhady, M. M., Youssef, A. M. TiO_2 nanowires and TiO_2 nanowires doped Ag-PVP nanocomposites for antimicrobial and self-cleaning cotton textile, Carbohydrate Polymers 91 549– 559 (2013).
13. Zhang, N., Liu, S., Fu, X., and Xu, Y. J. Synthesis of M@ TiO_2 (M= Au, Pd, Pt) core–shell nanocomposites with tunable photoreactivity. The Journal of Physical Chemistry C, 115(18), 9136-9145 (2011).
14. Epifani, M., Giannini, C., Tapfer, L., and Vasanelli, L. Sol–gel synthesis and characterization of Ag and Au nanoparticles in SiO_2, TiO_2, and ZrO_2 thin films. Journal of the American Ceramic Society, 83(10), 2385-2393 (2000).
15. Balek, V., Ŝubrt, J., Bountseva, I. M., Irie, H., and Hashimoto, K. Emanation thermal analysis study of N-doped titania photoactive powders. Journal of Thermal Analysis and Calorimetry, 92(1), 161-167

(2008).

16. Al-Sherbini, A. S. A., Ghannam, H. E., El-Ghanam, G. M., El-Ella, A. A., and Youssef, A. M. Utilization of chitosan/Ag bionanocomposites as eco-friendly photocatalytic reactor for Bactericidal effect and heavy metals removal. *Heliyon*, 5(6), e01980 (2019).

17. Barker, D. L., Hansen, M. S., Faruqi, A. F., Giannola, D., Irsula, O. R., Lasken, R. S., and Shen, R. Two methods of whole-genome amplification enable accurate genotyping across a 2320-SNP linkage panel. *Genome research*, 14(5), 901-907 (2004).

18. Thamaphat, K., Limsuwan, P., and Ngotawornchai, B. Phase characterization of TiO_2 powder by XRD and TEM.Kasetsart J. (Nat. Sci.), 42(5), 357-361 (2008).

19. Haroun, A. A., and Youssef, A. M. Synthesis and electrical conductivity evaluation of novel hybrid poly (methyl methacrylate)/titanium dioxide nanowires. Synthetic Metals, 161(19-20), 2063-2069 (2011).

20. Sun, S., and Zhang, F. Insights into the Mechanism of Photocatalytic Degradation of Volatile Organic Compounds on TiO_2 by Using In-situ DRIFTS. Semiconductor Photocatalysis: Materials, Mechanisms and Applications, 185 (2016).

21. Schauer, C. L., Chen, M. S., Chatterley, M., Eisemann, K., Welsh, E. R., Price, R. R., and Ligler, F. S. Color changes in chitosan and poly (allyl amine) films upon metal binding. Thin Solid Films, 434 (1-2), 250-257 (2003).

22. Wu, H. B., Hng, H. H., and Lou, X. W. Direct synthesis of anatase TiO_2 nanowires with enhanced photocatalytic activity. Advanced Materials, 24 (19), 2567-2571 (2012).

23. Wu, W. Q., Rao, H. S., Xu, Y. F., Wang, Y. F., Su, C. Y., and Kuang, D. B. Hierarchical oriented anatase TiO_2 nanostructure arrays on flexible substrate for efficient dye-sensitized solar cells. Scientific reports, 3, 1892 (2013).

24. Swetha, S., and Balakrishna, R. G. Preparation and characterization of high activity zirconium-doped anatase titania for solar photocatalytic degradation of ethidium bromide. Chinese Journal of Catalysis, 32(5), 789-794 (2011).

25. Tsuboi, M., Benevides, J. M., and Thomas Jr, G. J. The complex of ethidium bromide with genomic DNA: structure analysis by polarized Raman spectroscopy. Biophysical journal, 92(3), 928-934 (2007).